Heat and Mass Transfer 39 (2003) 345–353
DOI 10.1007/s00231-002-0320-0

Numerical Modeling of Film Cooling from Short Length Stream-Wise Injection Holes

A. Azzi, B.A. Jubran

Abstract This paper reports a numerical modeling and simulation studies of film cooling from stream-wise injection holes with various small hole length to diameter ratios, using a standard k-ε turbulence model with wall function. An anisotropic model was also applied in order to correct the deficit in lateral spreading of the k-ε model.

Comparisons of the present predicted results with experimental data and numerical results of previous studies show that using anisotropic turbulence model, multi-block grid techniques and extending the computational domain into the plenum supply of the injection holes tend to improve the prediction of the film cooling effectiveness especially at low blowing rates while for high blowing rates a more detailed description than the wall law approach is needed to describe the lift-off of the jet. Moreover, the film cooling protection is reduced as the hole L/d ratio is decreased.

List of symbols

d	diameter of the film cooling holes
k	turbulent kinetic energy
L	length of the hole
M	blowing ratio, $\rho_c U_c/\rho_\infty U_\infty$
p	streamwise spacing between rows of holes
S	spanwise spacing between holes
Tu	turbulence intensity
T	local temperature
$\bar{u}$	time-averaged velocity
u_i	velocities in the x_i-co ordinates direction
u', v', w'	velocities in x, y and z directions, respectively
X, x	Distance measured in the streamwise direction

Received: 29 June 2001
Published online: 5 July 2002
© Springer-Verlag 2002

A. Azzi
Université des Sciences et de la Technologie d'Oran,
Faculté de Mécanique, Département de Génie-Maritime,
B.P. 1505 El'mnaouar, Oran, ALGERIE

B.A. Jubran (✉)
Sultan Qaboos University, Department of Mechanical
and Industrial Engineering, Muscat, Sultanate of Oman
E-mail: bassamj@squ.edu.om

Greek

δ	boundary layer thickness
η	adiabatic film cooling effectiveness
ρ	Density
μ	dynamic viscosity
μ_t	turbulent eddy-viscosity
ε	rate of kinetic energy dissipation

Sub/Superscripts

p	plenum
∞	Free stream conditions
c	injection conditions

1 Introduction

Powerful gas turbine engines are characterized by high inlet temperature which results in a cooling requirement that necessities more effective techniques to cool the gas turbine blades. One such technique is the film cooling technique which is based on injection of the coolant air through simple and complex holes arranged in one or more rows of holes. For many years, investigators have been involved in developing and using various numerical procedures, turbulence models and grid techniques to predict the film cooling thermal and hydrodynamic fields.

Numerous investigations have been carried out on numerical prediction of film cooling from various configurations of holes that varies in complexity, such as those reported by Jubran [1], Amer et al. [2], Demuren [3] and Zhou et al. [4]. These studies do not take into account the flow inside the injection hole and do not include the length of the injection hole into the computational domain. The boundary conditions are applied by setting constant velocity or constant pressure at the injection exit hole. As it is found by Andreopouls [5] the flow inside the hole is widely perturbed by the mainstream flow, especially for low blowing ratio. Assuming a uniform flow at the exit of the hole is not very accurate and a good numerical model must include the hole space in the computational domain. In order to simulate correctly the characteristics of jets in a cross-flow issuing from a row of holes, Theodoridis et al. [6] used a computational grid taking into account the hole domain until 20 times the diameter. A multi-block technique with a fully elliptic procedure has been used by Lakehal et al. [7] to predict a film cooling by lateral

injection. This technique generates different grids for different parts of interest, namely the region above the flat plate and the discharge pipe, which are finally linked to form the complete computational domain. Azzi et al. [8] predicted film-cooling characteristics from compound angle injection holes using a standard k-ε turbulence model. Their computational domain includes the length of the injection holes.

Film cooling holes used in gas turbine airfoil applications are designed with small-hole length-to-diameter ratio with coolant to mainstream density ratio of 2, Leylek and Zerkle [9]. Numerical prediction for such types of holes using three dimensional Navier-Stokes equations seems to be limited in the open literature with the exception of the works of Theodoridis et al. [6], Lakehal et al. [7] and Leylek and Zerkle [9] who extended the computational domain into the injection hole and into the plenum itself for the small film-hole length-to-diameter ratio. Moreover, they reported that the lateral spreading of the jet is underpredicted if no special handling was made to the standard k-ε turbulence model, which is the mostly used one.

Recently, Leylek & Zerkle [9], Walters & Leylek [10, 11], and Ferguson et al. [12] presented detailed computational studies and conclude emphatically the fact that before reaching any conclusions related to the ability of any turbulence model to predict the thermal and hydrodynamics fields of film cooling, the numerical approach must follow the four critical issues of computational simulation. These are: (1) proper computational modeling of flow physics; (2) exact geometry and high quality grid generation; (3) higher order discretization scheme; and (4) effective turbulence modeling. In the first study, Leylek and Zerkle [9] uses an elliptic Navier-Stokes code with a structured mesh, a first order discretization scheme (hybrid) and the standard k-ε model with wall function to compute numerically the film cooling from one row of 35 deg hole. The main feature of Leylek and Zerkle's paper is to include the plenum supply in the computational domain, which permits a realistic application of the boundary conditions and fulfills the requirement of the first issue. Leylek and Zerkle's paper was followed by a series of papers, Walters & Leylek [10, 11] which satisfies the first three issues by using a commercial code called Fluent. In another paper, Ferguson et al. [12] presented a comparison between the performance of various turbulence models (standard k-ε, RNG k-ε, and RSM) and near-wall treatments (Wall Functions and Two-layer Zonal Model). The references cited above document in detail the strong coupling interaction between the flow field in cross flow, the injection hole and the plenum supply. A novel vorticity based approach was also included in the analysis to obtain a clearer picture of the flow physics. The two-layer model was found to be the most appropriate one to describe the jet-off occurring immediately after the hole, but it is also very costly in time computing (one week versus one day for wall function approach, Ferguson et al., [12]. If we retain the wall function approach, the standard k-ε model was judged to be the most appropriate to reproduce results that are more consistent with experimental data. It must be pointed out that Leylek and Zerkle [9] used a single-block structured grid procedure which made it difficult to maintain a refined high-quality grid in the jet exit region. On the other hand, Walter and Leylek [10] used an unstructured grid procedure.

In the present investigation, a multi-block structured grid was used to maintain a refined high-quality grid in the jet exit region. Furthermore, a second-order bounded scheme for the convective terms was used to allow its application for all governing equations including those of k and ε. The anisotropic model proposed by Bergeles et al. [13] was also applied in order to correct the deficit in lateral spreading of the k-ε model. A fully vectorized three-dimensional finite-volume technique with complex boundaries was applied to predict film cooling in configurations relevant to gas turbine blades that have small-hole length-to diameter ratio and a density ratio of coolant to mainstream of 2. The standard k-ε model with the anisotropic model of Bergeles et al. [13] was used to allow for the right lateral spreading of the jet.

The common features of this work compared with that of Leylek and Zerkle [9] are the use of fully coupled and elliptic computation of flow in plenum, film-hole and cross-stream regions of the film cooling field as well as a highly orthogonalized grid. The originality of the present study in comparison with the work of [9] is the use of multi-block structured strategy that significantly reduces the core memory needed and gives more freedom in the generation of the grids. In addition to that, the use of a second order accurate bounded scheme for convective terms, which allows grid independence for relatively small number of nodes as well making use of Bergeles et al. model [13] to account for the lateral spreading of the jets. The predicted results are compared with the experimental results of Sinha et al. [14] and previous computational results of Leylek and Zerkle [10]. Moreover, extending the work of Lutum and Johnson [15] by detailed prediction of the flow inside the hole and in the vicinity of the entrance and the exit of the injection for various hole length-to-diameter ratios.

2 Computational Approach

2.1 Mathematical Formulation

The mathematical film-cooling model consists of the RANS (Reynolds Averaged Navier Stokes equations), the energy equation and the standard k-ε model with wall function. Details of the mathematical formulation can be found in references [16, 17]. In this study, boundedness is achieved by way of van Leer's MUSCL (Monotonic Upstream Scheme for Conservation Laws [18]) approach.

The MUSCL scheme may be written in terms of canonical representation as follows:

$$\phi_e = \phi_P + \frac{1}{4}\left[(1-\kappa)\bar{\Delta}_e^- + (1+\kappa)\tilde{\Delta}_e\right] \quad U_e > 0 \qquad (1)$$

$$\phi_e = \phi_P + \frac{1}{4}\left[(1-\kappa)\tilde{\Delta}_e^+ + (1+\kappa)\bar{\Delta}_e\right] \quad U_e < 0 \qquad (2)$$

where ϕ_e is the expression of convective scalar and U_e is the flow velocity, both at east control volume face. The following difference operators are defined

$$\bar{\Delta}_e^- = \min\mathrm{mod}\left(\Delta_e^-, \omega\Delta_e\right) \quad \tilde{\Delta}_e = \min\mathrm{mod}\left(\Delta_e, \omega\Delta_e^-\right) \tag{3}$$

$$\bar{\Delta}_e = \min\mathrm{mod}\left(\Delta_e, \omega\Delta_e^+\right) \quad \tilde{\Delta}_e^+ = \min\mathrm{mod}\left(\Delta_e^+, \omega\Delta_e\right) \tag{4}$$

$$\Delta_e = \phi_E - \phi_P; \quad \Delta_e^- = \phi_P - \phi_W; \quad \Delta_e^+ = \phi_{EE} - \phi_E \tag{5}$$

where P, W, E and EE are the centers of the central, west, east and far-east calculation control volumes. The Quadratic Upstream Interpolation for Convective Kinematics bounded scheme (QUICK) can be created by setting κ to 1/2.

The minmod function is defined in the way to return the argument with minimum absolute value if both arguments have the same sign and return zero otherwise.

$$\min\mathrm{mod}(A, \omega B) = sgn(A)\max\{0, \min\{|A|, \omega B sgn(A)\}\} \tag{6}$$

with ω a compression parameter determined in the range given by

$$1 \le \omega \le (3-\kappa)/(1-\kappa) \tag{7}$$

Normally, it is advised to use the maximum allowable value, which is in our study $\omega = 5$ since $\kappa = 1/2$.

2.2 Numerical Procedure

The numerical procedure used to calculate the test case is based on a finite-volume approach for implicitly solving the incompressible averaged Navier-Stokes equations on multi-block arbitrary non-orthogonal grids, employing a cell-centred grid arrangement. The momentum-interpolation technique of Rhie and Chow [19] is used to prevent pressure-field oscillations and the pressure-velocity coupling is achieved using the SIMPLEC algorithm of Van Doormal and Raithby [20]. The resulting system of the algebraic difference equations is solved using the Strongly Implicit Procedure (SIP) of Stone [21]. The convection fluxes are approximated by a second-order bounded scheme, namely the MUSCL (Monotonic Upstream Scheme for Conservation Laws) of Van Leer [18]. The fluid density is calculated as a function of the temperature via the state equation.

In order to account for the anisotropy of the turbulent exchange processes in these flows, Bergeles et al. [13] proposed to substitute the eddy-viscosity μ_t appearing in the lateral components of the Reynolds stresses and scalar fluxes:

$$-\overline{u'w'} = \frac{\mu_t}{\rho}\frac{\partial u}{\partial z}; \quad -\overline{w'\theta'} = \frac{\mu_t}{\rho\,\mathrm{Pr}_t}\frac{\partial T}{\partial z} \tag{8}$$

by an increased value determined by

$$\mu_t^a = \mu_t[1.0 - f(1.0 - y/\delta)] \tag{9}$$

in which μ_t is the eddy viscosity determined by the basic turbulence model. δ denotes the local boundary layer thickness. Relation (8) was derived from model transport equations for the Reynolds stresses by assuming local equilibrium of turbulence and neglecting the stress $\overline{v'w'}$ against $\overline{u'v'}$ and $\overline{u'w'}$. The ratio of eddy viscosities/diffusivities for the stresses and heat fluxes in the lateral and normal was found to be equal to the ratio of the fluctuating velocities $\overline{w'^2}/\overline{v'^2}$, which was assumed to vary linearly from a near-wall value f to 1 at the outer edge of the boundary layer. The coefficient f was given the value 3.5 in Bergeles et al. [13].

2.3 Film Cooling Geometry, Grid and Boundary Conditions

The Film cooling geometry and the experimental conditions predicted in the present paper are similar to that used by Walters and Leylek [10, 11] which are basically that of Pietzryk et al. [22, 23], Sinha et al. [14] and are illustrated in Figure 1 together with the Cartesian coordinate system and the bounding planes of the computational domain. In addition to that the hole length-to diameter ratio was varied from 1.75 to 8 to predict its effect on film cooling thermal and hydrodynamic fields. The overall extent of the cross stream computational domain in the streamwise, vertical, and lateral directions is 49D, 10D, and 1.5D, while the plenum is 8D, 4D, and 1.5D, respectively. The pitch to diameter ratio (P/d) in the spanwise direction is 3, and the holes are inclined at 35 degrees with respect to the test surface. The film hole diameter is 12.7 mm.

The quality of a computational solution is strongly linked to the quality of the grid mesh. So a highly orthogonalized, nonuniform, multi-block fine grid mesh was generated with grid nodes considerably refined in the near-wall region and in the inlet and the exit hole vicinity. The normalized y^+ values at the near wall node are kept within $12 < y^+ < 60$, and care is taken so that the stretching factors are kept close to unity. Similarly, the grid aspect ratio was kept well under 18 in the entire computational domain. A total of 185,265 grid nodes (disposed on a global array 179×45×23 nodes in x, y, and z directions) were used with 89.5% of active nodes, which gives exactly 165,766 nodes. We note here, although the grid used by Leylek and Zerkle [9] is composed of 200,090 grid nodes, yet because of the excessive blocked nodes used in the single-block grid, the active nodes were not greater than 128,000. The multi-block grid method used in this study reduces significantly the number of inactive nodes. The grid generated is composed of three blocks, which are the domain over the flat plate for the first block, the injection

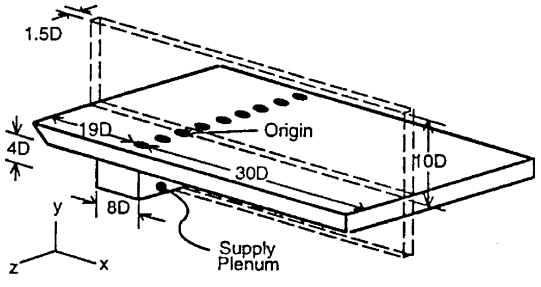

Fig. 1. Experimental film cooling configuration, computational domain and coordinate system, (Walters and Leylek, 1997)

tube for the second and the plenum for the third one. Grid sizes of 108×42×23, 16×40×16, and 53×42×23 grid points are used for the first, second and third blocks respectively.

Figure (2) shows the multi-block grid used for L/d=8.0. The semi-elliptic cross section plane of the round film-hole was transformed into a purely orthogonal rectangle within a short distance above and below the test plate.

Boundary conditions are prescribed at all boundaries of the computational domain by imposing exactly the measurements made in experiments. Mainstream conditions were kept the same in all cases and the coolant flow rate was altered to change the blowing ratio in such a way to be fully consistent with the procedure described by Sinha et al. [14] and used by Leylek and Zerkle [9]. Symmetry conditions are used for the two lateral planes in the first and the third blocks, and in one side of the second block. The top surface for block 1 is also considered as symmetry plane because it is sufficiently far from the test plate. The velocity profile at the inlet plenum, which is at the bottom surface of block 3 is determined in such a way to produce the desired blowing ratio and the density ratio at the known plenum temperature (T_p) of 153 K. The remaining two components of the velocity were set to zero, and assuming a condition of local equilibrium, uniform distributions of k and ε were computed from the velocity. The turbulence intensity was set to 2 percent, and length scale was taken to be equal to 1/10 of plenum width.

At the mainstream inflow boundary in block 1, a streamwise velocity of 20 m/s was specified to produce the desired mainstream Reynolds number at the measured cross-flow temperature (T_{inf}) of 302 K. The remaining two components of the inlet velocity vector were set to zero. The k and ε profiles are specified using uniform distributions corresponding to a free-stream turbulence intensity of 2%, and a turbulence length scale equal to 1/10 of computational passage height. At the outflow boundary, the gradients of all flow variables with respect to the streamwise direction were set to zero, and the no-slip condition with wall function approach were applied at the solid walls. All walls are considered thermally adiabatic.

The fully converged solution obtained from the lowest blowing ratio (M=0.5) case was used as the initial field for the next case with a modified velocity component, k, ε and viscosity (only in plenum and in injection tube) to match with the new blowing ratio. The normalized residual was computed over all the computational nodes and was normalized by the total inlet flux (crossflow and plenum combined) of relevant quantity for each equation. The computational solution was declared "fully converged" when the normalized residual of each governing equation was at or below 1 percent level, overall mass imbalances of less than 0.01%, no change in temperature distribution in each 50 iterations, and all residual levels were reduced approximately three orders of magnitude depending on the initial conditions. The computations did not display any convergence difficulties, which are achieved after approximately 1500 iterations on a micro-computer (PIII, 450Mhz, 128M of memory) in slightly less than one full day.

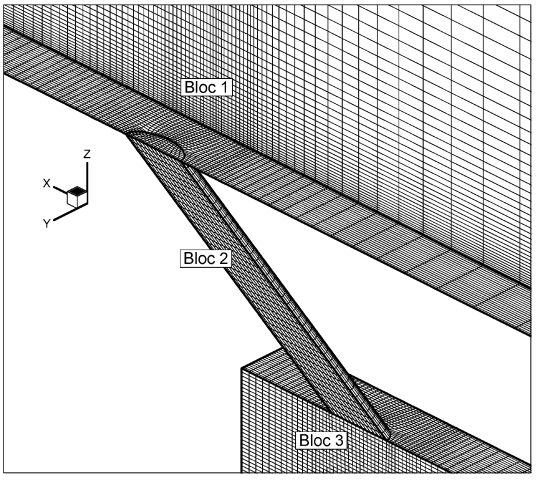

Fig. 2. The computational grid, L/d=8.0

3 Results and Discussion

Comparisons between the predicted results of the film cooling effectiveness, $\eta = (T - T_\infty)/(T_c - T_\infty)$, at the centerline of the jet using the standard k-ε (SKE) and the Bergeles modification (KEB), and the experimental results of Sinha et al. [14] are shown in Figure 3 (a, b). The lateral averaged adiabatic film cooling effectiveness distributions are shown in Figure 4 (a, b). Moreover, the present predicted results are also compared with the previous

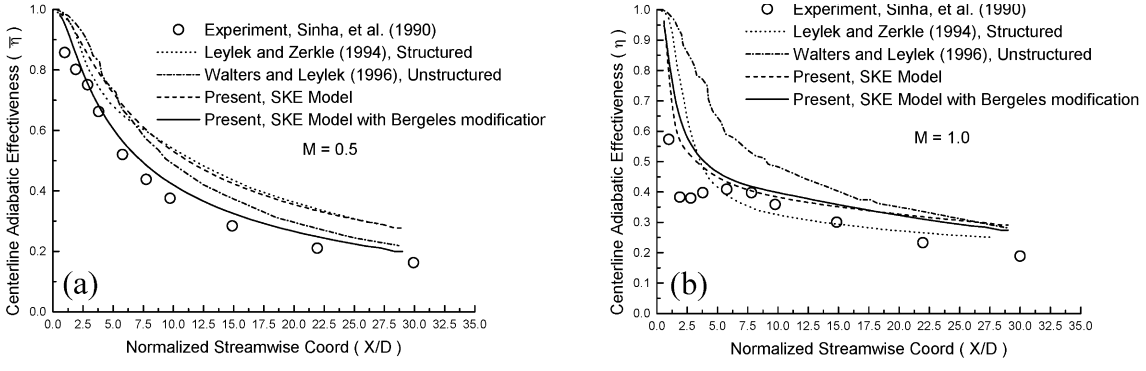

Fig. 3. Streamwise variation of the centerline adiabatic effectiveness, (a): M=0.5, (b): M=1.0

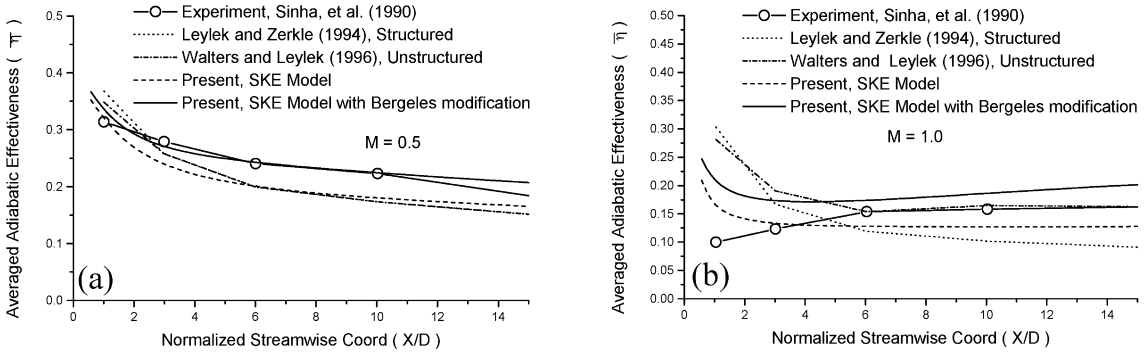

Fig. 4. Laterally averaged adiabatic effectiveness, (a): M=0.5, (b): M=1.0

computed results of Leylek and Zerkle [9] and Walters and Leylek [10], in Figures 3 and 4 and are shown as LZ94 and DL96, respectively. It must be pointed out that in this comparative study we don't take into account the correction made by Walters and Leylek [10] in order to correct the skewing of the coolant jets downstream of the film-hole observed experimentally. This is due to the fact that the skewness angle is roughly estimated by Walters and Leylek [10] as equal to 1.5°. It was clearly indicated in their paper that this value (1.5°) should not be considered as the "right" one.

It can be seen clearly from Figure 3(a) that the present *SKE* values for M = 0.5 are approximately collapsed with those of LZ94. Small deviations between the present predicted results and the experimental ones are observed in the vicinity of the holes at X/d < 2.0, while far downstream the two results are identical. It also appears that the results with Bergeles modification are improved as compared with those of SKE model. This fact is explained by the lateral spreading which results in a less centerline effectiveness and more lateral averaged adiabatic effectiveness as it is shown in Figure (4, a) and Figure (5). The slight over-prediction noted far downstream can simply be explained by the skewness of the jet as cited in Walters and Leylek [10]. It is also noted that there is almost a perfect agreement between the laterally averaged adiabatic effectiveness experimental results and KEB predictions, especially at X/d = 6 and 10, Figs. (4, a–b).

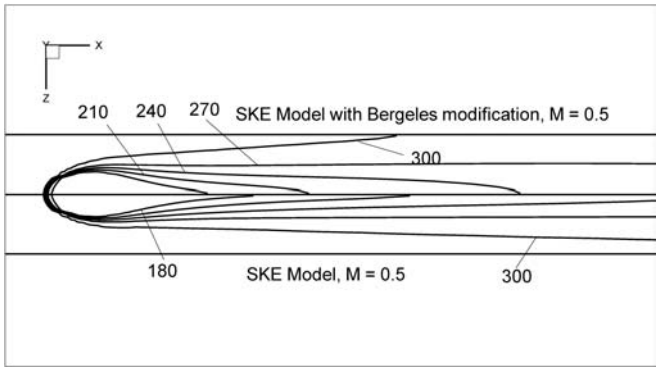

Fig. 5. Temperature contours on the bottom wall, M=0.5

For M=1.0, no one of the present or previous computed results are able to capture the detachment-reattachment of the jet represented in experimental curve by the sudden fall of centerline effectiveness near the trailing edge. It was also demonstrated in a recent study by Ferguson et al. [12] that the size of detachment-reattachment is too small and can not be captured by the wall law approach, since in the near wall treatment, the position of the first center of the control volume must verify ($y^+ > 11.6$).

The improvement of the KEB predicted results in comparison with SKE model is clearly shown in Figure (6), where predicted lateral variations of η are presented as well as the measured ones. Measured data indicate non-zero η values at the mid-pitch location (Z/d=1.5) for all lateral profiles except for that at X/d=1. Computed η curves with SKE model, show almost zero effectiveness beyond Z/d=1.0 for the first three stream-wise locations, $1 \leq X/D \leq 6$, and also beyond Z/d=1.2 at X/d=15. The KEB model shows more lateral spreading resulting in a nonzero values at Z/d=1.5 and much improved values at Z/d=0. The same low rate of spreading with SKE model is found by Walters and Leylek [10].

The complex nature of the flow is highlighted by results plotted on planes perpendicular to cross-flow (X/d = 5) as it is shown in Figure (7). The flow is characterized by the counter-rotating vortex structure. The strength of secondary flow, the vertical and lateral locations of the core center are directly related to the blowing ratio. For high blowing ratio (M=1.0) the vertical location and the distance between the two vortex are bigger than those obtained for low blowing ratio (M=0.5). As it is explained by Walters and Leylek [11], the lower value of the vertical position reduces their lift and convective strength, since the wall participates to realigning the secondary flow. The small distance between the two vortices increases their convective strength.

Computed velocity vectors on the centerline plane of the film-hole are presented in Figure 8 for M=0.5 and M=1.0. The short coolant supply tube is characterized by a low momentum region near the downstream wall and a jetting effect near the upstream wall, which is stronger at high blowing ratio (M=1.0). Hence, it is more accurate to include the plenum supply in computational domain than simply applying an exit profile in the inlet tube. It is also expected that for a high value of length to diameter ratio

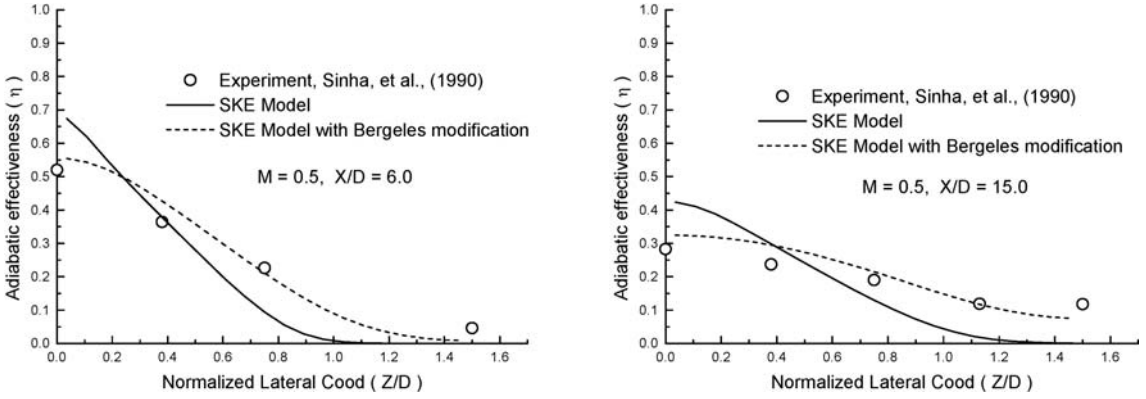

Fig. 6. Lateral variation of adiabatic effectiveness at different stations downstream of the hole injection

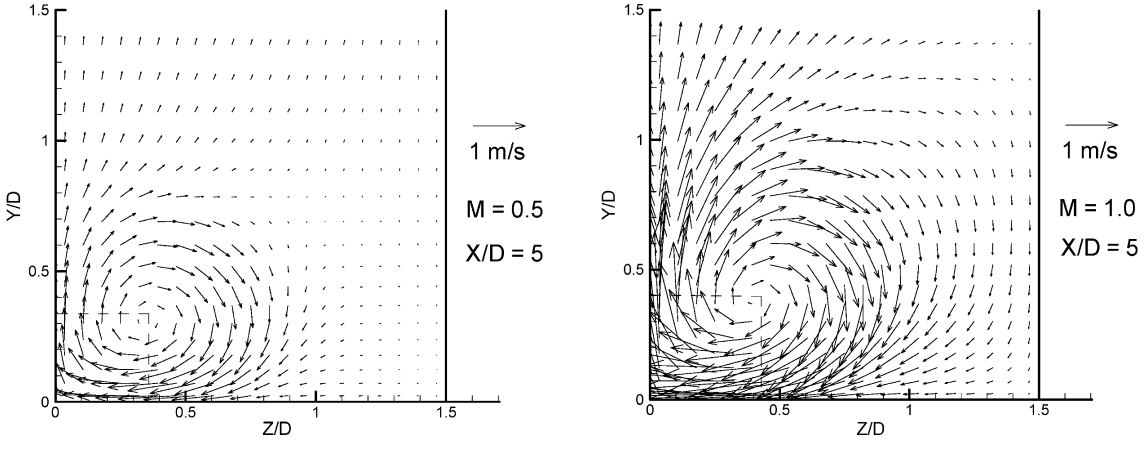

Fig. 7. Velocity vectors on spanwise plane. X/d=5

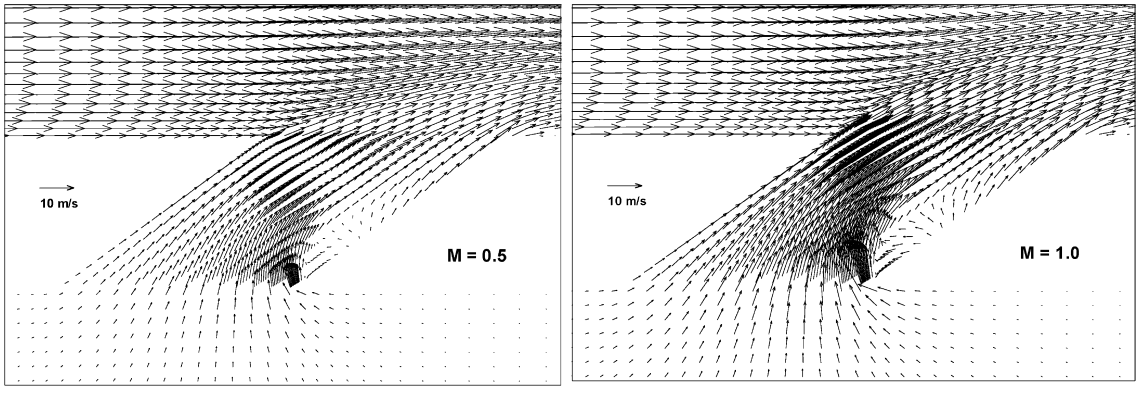

Fig. 8. Velocity vectors on centerline plane in the film-hole region

this phenomena has a negligible influence on cross-stream flow. At it was hypothesized by Pietrzyk et al. [23] there is a separation region within the film-hole itself which is responsible for the shape of the velocity profiles and high turbulence intensities at the exit plane of the film-hole.

The effect of the coolant hole length-to-diameter ratio on the adiabatic film cooling effectiveness along the jet centerline as well as the laterally averaged film cooling effectiveness for M=0.5 and 1.0, and L/d=1.75, 3.5, 5 and 8, is shown in Figures 9 and 10. The inability of the SKE model to capture the exact values of the adiabatic effectiveness was already highlighted by Leylek et al. [9] and recently by Azzi et al. [8]. Nevertheless, the qualitative trend is well captured specially for low blowing ratio. In a previous study, Azzi and Lakehal [24] show that the jet lift-off and reattachment occurring immediately downstream of the jet, are characterized by the sudden decrease in effectiveness and cannot be captured by the wall function procedure. More elaborate models such as that of Bergeles anisotropic modification and the two-layer procedure may

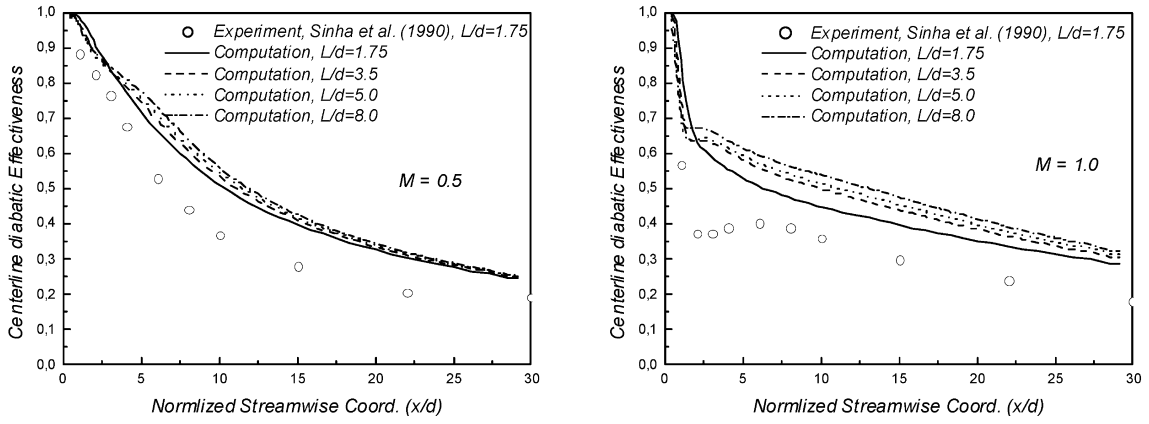

Fig. 9. Centerline adiabatic effectiveness

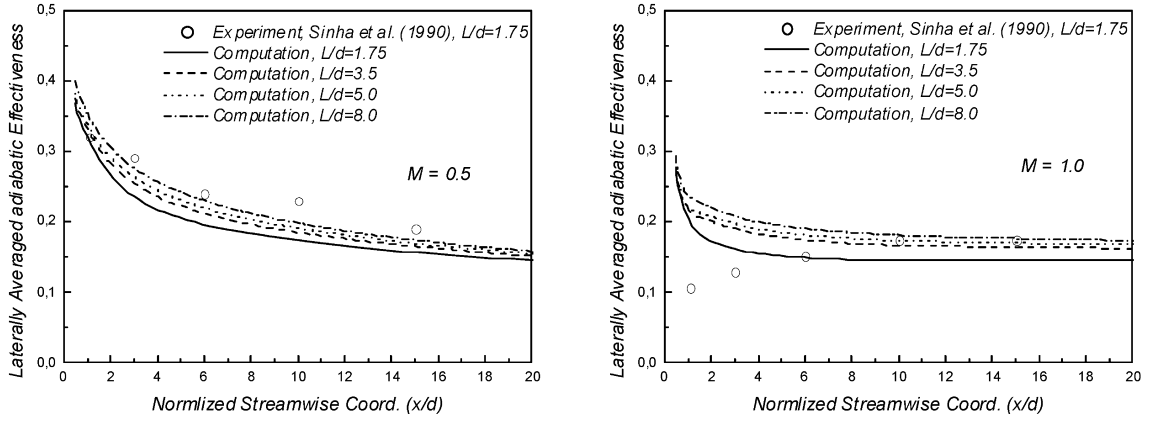

Fig. 10. Laterally averaged adiabatic effectiveness

perform better in such cases. In order to have a parametric study where the influence of the length to diameter ratio on the film cooling effectiveness is investigated in a way free of any modifications, the standard k-ε model is used in the present study.

It can be seen from Figure 9 that for both blowing ratios (M=0.5 and 1.0), the predicted film cooling effectiveness values for L/d=1.75, and at the vicinity of the injection holes are slightly bigger than those obtained for the other length-diameter ratios. With increasing distance downstream, (x/d >3) lower effectiveness values are obtained with the shorter injection holes with the effect more pronounced for M=1.0. The film cooling effectiveness increases with increasing hole L/d ratio. It is also interesting to note that at M=1.0 and L/d=1.75, the jet lift-off is captured immediately downstream the jet location. Similar trends on the effect of L/d on the film cooling effectiveness have been reported experimentally by Lutum and Johnson [15]. Figure 10 shows that the effect of L/d on the laterally averaged adiabatic film cooling effectiveness is more evident.

When comparing the turbulence intensity contours for different L/d ratios in Figure 11, it can be seen that the turbulence levels are significantly different. In the plenum the velocities are extremely small except in the vicinity of the film-hole entrance, where the fluid accelerates and enters the film hole. The complex and undeveloped flow

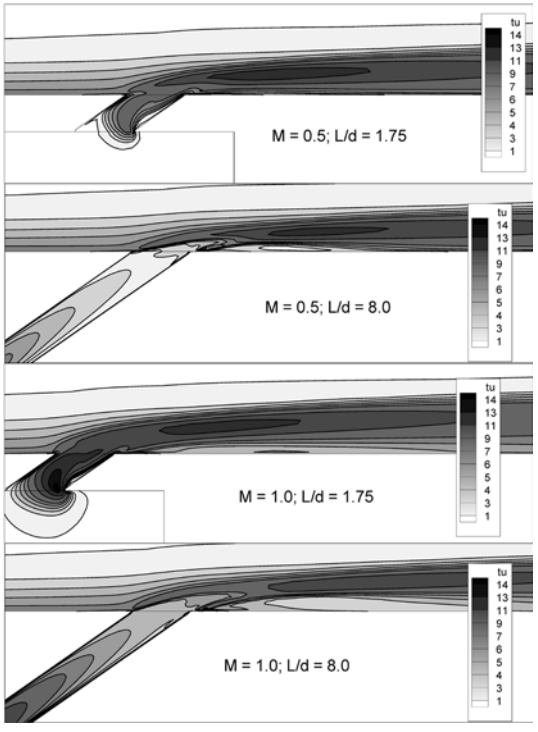

Fig. 11. Turbulence intensity contours at mid-plane through the injection hole

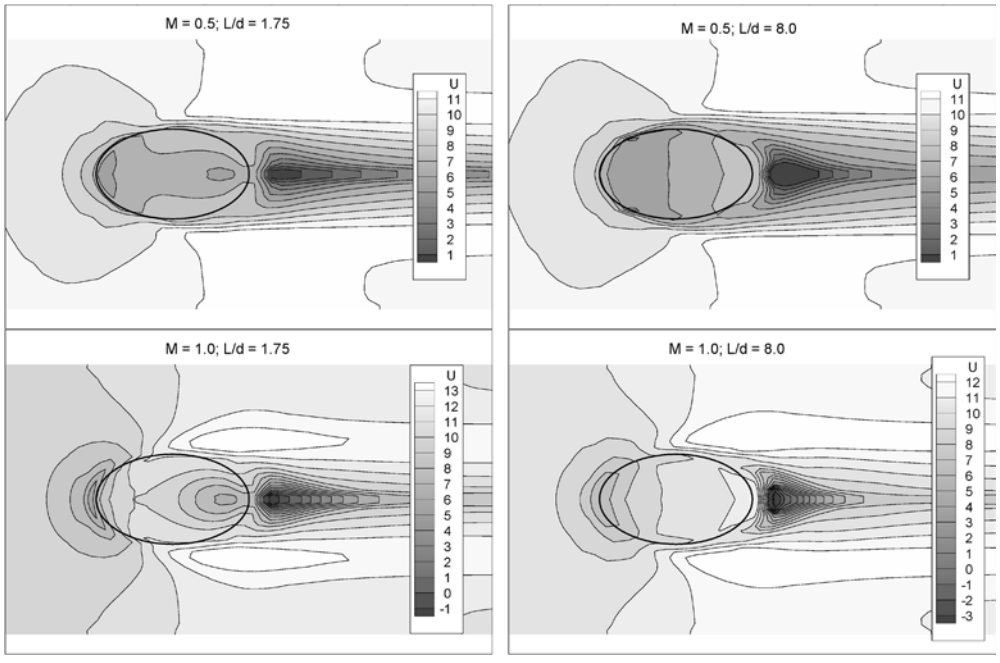

Fig. 12. Streamwise velocity contours over the flat plate

inside the hole results in a high level of turbulence, which is still present at the exit for the short hole. For the long hole (L/d=8) a lower turbulence level is present at the exit of the hole and also under the jet. We can also, see that a higher level of turbulence (14% for M=1.0 and 11% for M=0.5) is present inside the hole for high blowing ratio and in the jet for the low blowing ratio.

Figure 12, shows the longitudinal velocity contours on the flat plate and in the vicinity of the hole injection for different blowing ratios and different hole length. For the low blowing ratio (M=0.5) the zone of small velocity downstream the hole injection is bigger for L/d=8. The contour lines inside the hole itself are also very different. For (L/d=8) case the coolant leaves the hole mainly from the upstream part where for (L/d=1.75) it leaves the hole from the lateral boundaries. This is true especially for the undeveloped flow character at L/d=1.75, and the fully duct developed flow character at L/d=8. This is also true for high blowing ratio, with a development of an acceleration zone on either side of the hole injection. It is useful to note that the interaction between the jet and the mainstream flow can be compared to solid cylinder in a cross flow. The flow presents a high-pressure level upstream the jet and low-pressure level downstream the jet while the flow between the holes is normally accelerated.

4 Conclusions

A Systematic Computational approach based on anisotropic turbulence model, multi-block grid techniques and extending the computational domain into the plenum supply of the injection holes has been used to predict film cooling from streamwise injection holes with different small hole length to diameter ratio. It was found that such an approach tends to improve the prediction of the film cooling effectiveness especially at low blowing rates. Moreover, the numerical modeling of the injection holes must include the plenum supply in computational domain rather than simply applying an exit profile in the inlet tube in order to increase the accuracy of the predicted results, especially for low values of hole length to diameter ratios. In addition to that an alternative to the wall law approach must be developed to accurately model the lift off of the jet at high blowing rates.

The ability of the standard k-ε turbulence model with Bergeles modification, KEB to predict the thermal and hydrodynamic characteristics of film cooling fields is very much dependent on the blowing ratio and the distance downstream the injection holes. It was also found that for a blowing ratio, M=0.5 the main source of turbulence is the shear layer between the cross-flow and the coolant jet while for the high blowing ratio (M=1.0) the main source of turbulence is in the film-hole itself.

References

1. Jubran, B. A. (1989) Correlation and prediction of film cooling from two rows of holes. ASME Journal of Turbomachinery 111: 502–509.
2. Amer, A. A.; Jubran, B. A.; Hamdan, M. A. (1992) Comparison of different two-equation turbulence models for prediction of film cooling from two rows of holes. Numerical Heat Transfer, Part A, 21: 143–162.
3. Demuren, A. O.; Rodi, W.; Schonung, B. (1986) Systematic study of film cooling with a three-dimensional calculation procedure. ASME Journal of Turbomachinery 108: 124–130.
4. Zhou, J.; Salcudean, M.; Gartshore, I. S. (1993) Prediction of film cooling by discrete-hole injection. ASME paper 93-GT-75.
5. Andreopoulos, J. (1982) Measurements in a jet-pipe flow issuing perpendicularly into a cross stream. ASME Journal of Fluid Engineering 104: 493–499.
6. Theodoridis, G. S.; Jubran, B. A.; Rodi, W. (1997) Numerical prediction of flow characteristics of jets in a cross-flow issuing from a row of holes, JSME Conference, Tokyo.
7. Lakehal, D.; Theodoridis, G. S.; Rodi, W. (1997) Computation of film cooling by lateral injection using a multi-block technique. Proc. 11th Turbulent Shear Flow Symposium, Grenoble, Sept. 8–10, 1997.
8. Azzi, A.; Abidat, M.; Jubran, B. A.; Theodoridis, G. S. (2001) Film Cooling Predictions of Simple and Compound Angle Injection From One and Two Staggered Rows. Numerical Heat Transfer, Part A, 40: 273–294.

9. Leylek, J. H.; Zerkle, R. D. (1994) Discrete-Jet Film Cooling: A Comparison of Computational Results With Experiments. ASME Journal of Turbomachinery 116: 358–368.
10. Walters, K. D.; Leylek, J. H. (1996) A Systematic Computation Methodology Applied to a Three-Dimensional Film-Cooling Flowfield. ASME 96-GT-351.
11. Walters, K. D.; Leylek, J. H. (1997) A Detailed Analysis of Film-Cooling Physics, Part I: Streamwise Injection With Cylindrical Holes. ASME 97-GT-269.
12. Ferguson, D. J.; Walters, K. D.; Leylek, J. H. (1998) Performance of Turbulence Models and Near-Wall Treatments in Discrete Jet Film Cooling Simulations. ASME 98-GT-438.
13. Bergeles, G.; Gosman, A. D.; Launder, B. E. (1978) The Turbulent Jet in a Cross Stream at Low Injection Rates: A Three-Dimensional Numerical Treatment. Num. Heat Transfer 1: 217–242.
14. Sinha, A. K.; Bogard, D. G.; Crawford, M. E. (1990) Film-Cooling Effectiveness Downstream of a Single Row of Holes With Variable Density Ratio. ASME Journal of Turbomachinery 113: 442–449.
15. Lutum, E.; Johnson, B. V. (1999) Influence of the Hole Length-to-Diameter Ratio on Film Cooling with Cylindrical Holes. ASME Journal of Turbomachinery 121: 209–216.
16. Majumdar, S.; Rodi, W.; Zhu, J. (1992) Three-Dimensional Finite-Volume Method for Incompressible Flows With Complex Boundaries. ASME Journal of Fluids Engineering 114: 496–503.
17. Zhu, J. (1992) An Introduction and Guide to the Computer Program FAST3D. Report No. 691, Institute for Hydromechanics, University of Karlsruhe.
18. Leonard, B. P. (1991) The ULTIMATE conservative difference scheme applied to unsteady one-dimensional advection. Comp. Math. Appl. Mech. Engineering 88: 17–74.
19. Rhie, C. M.; Chow, W. L. (1983) A Numerical Study of the Turbulent Flow Past an Isolated Airfoil with Trailing Edge Separation. J. AIAA 21: 1225–1532.
20. Van Doormal, J. P.; Raithby, G. D. (1984) Upstream to Elliptic Problems Involving Fluid Flow. Computers and Fluids 2: 191–220.
21. Stone, H. L. (1968) Iterative Solution of Implicit Approximation of Multidimensional Partial Differential Equations. SIAM J. on Num. Analysis 5: 53.
22. Pietrzyk, J. R.; Bogard, D. G.; Crawford, M. E. (1988) Hydrodynamic Measurements of Jet in Cross-flow for Gas Turbine Film Cooling Applications. ASME Paper No. 88-GT-194.
23. Pietrzyk, J. R.; Bogard, D. G.; Crawford, M. E. (1989) Effect of Density Ratio on the Hydodynamic of Film cooling. ASME Paper No. 89-GT-175.
24. Azzi, A.; Lakehal, D. (2001) Perspectives in Modeling Film-Cooling of Turbine Blades by Transcending Conventional Two-Equation Turbulence Models. Proc. ASME/IMECE 2001, New York, Nov. 11–16 (2001).